

Single pulse all-optical toggle switching of magnetization without Gd: The example of Mn_2Ru_xGa

C. Banerjee, N. Teichert, K. Siewierska, Z. Gercsi, G. Atcheson, P. Stamenov,
K. Rode, J. M. D. Coey and J. Besbas*

¹ CRANN, AMBER and School of Physics, Trinity College, Dublin 2, Ireland

*besbasj@tcd.ie

Viable and energy-efficient control of magnetization without the help of a magnetic field is a key goal of spintronics^{1,2}. Purely thermal single-pulse all-optical toggle switching has been demonstrated, but so far only in Gd based amorphous ferrimagnet films³⁻⁶. In this work, we demonstrate thermal single-pulse toggle switching in the half-metallic compensated ferrimagnetic Heusler alloy Mn_2Ru_xGa with crystallographically- inequivalent Mn sublattices⁷. Moreover, we find single-pulse switching in samples with compensation temperatures above room temperature that are immune to external magnetic fields in excess of 1 T. Observation of the effect in alloys with no f shell moments challenges our understanding of all-optic switching. The findings widen the basis for fast optical switching of magnetization and break new ground for engineered materials that can be used for controlled data writing with ultrashort pulses of light.

Driven by the demands for high speed, low cost and high-density magnetic recording, research in spintronics has always sought insight into new classes of magnetic materials and devices that show efficient and reproducible magnetization switching. In this regard, interest

in the magnetic properties in antiferromagnetically coupled sub-lattice systems has gained momentum in the last decade. The total or partial cancellation of the moments makes these systems insensitive to stray magnetic fields, and the interaction between the sublattice moments introduces phenomena that are absent in conventional ferromagnetic systems, opening new opportunities for magnetic recording and information processing^{2,8-10}. An efficient way of controlling magnetism is to use ultrashort laser pulses^{1,11}. A basis for thermal single-pulse all-optical switching (SP-AOS) of the magnetization of a thin layer of amorphous $\text{Gd}_{25}\text{Fe}_{65.6}\text{Co}_{9.4}$ with perpendicular magnetic anisotropy was described by Radu *et al.*³. Amorphous $\text{Gd}_x(\text{Fe},\text{Co})_{100-x}$ with $x \approx 25$ is a metallic ferrimagnet with localized $4f$ -shell magnetic moments in the Gd sublattice and delocalized $3d$ -band moments in the Fe-Co sublattice. Upon excitation by a femtosecond laser pulse, the Fe-Co undergoes sub-picosecond demagnetization leading to a nearly complete loss of the ordered $3d$ shell moment, an effect that had been originally observed in ferromagnetic nickel¹². Concomitantly, the Gd sublattice experiences a slower loss of its magnetic moment driven by a spin-conserving charge transfer from the f shell to the FeCo d shell³, ensuring a transient parallel alignment of the weak magnetizations of the Gd and demagnetized FeCo sublattices that ultimately leads to magnetization toggle switching on a picosecond timescale^{3,13}. As the suggested mechanism of SP-AOS relies on an ultrafast interplay between magnetized d and f states in a multisublattice system, it was expected that it should be found in rare-earth based ferrimagnets only¹⁴. In practice however, SP-AOS has only been demonstrated in ferrimagnetic $\text{Gd}_x(\text{Fe},\text{Co})_{100-x}$ thin³, $\text{Gd}_x(\text{Fe},\text{Co})_{100-x}$ spin valves⁵ and in synthetic Gd/Co ferrimagnets⁴; It has not been identified in other rare-earth based ferrimagnet such as amorphous $\text{Tb}_{27}\text{Co}_{73}$ ¹⁵ where the $4f$ electrons experience strong spin-orbit coupling. Its thermal origin is established by the independence of the effect on the helicity of the light^{3,13},

and the equivalent effect produced by pulses of hot electrons¹⁶. Here by thermal, we understand that the electrons can be assigned a distribution characterized with a temperature but not necessarily the equilibrium temperature. A related effect has been reported in ferromagnetic Pt/Co/Pt structures, but only when the laser spot size matches that of the ferromagnetic domains¹⁷. Non-thermal, single-pulse, non-toggle switching has been reported with linearly-polarized light in insulating Co-doped yttrium iron garnet¹⁸.

In the present work, we show that the inclusion of a rare-earth element is not required to observe SP-AOS. We report all-optical toggle switching in the ferrimagnetic Heusler alloy $\text{Mn}_2\text{Ru}_x\text{Ga}$ (MRG)⁷ where both magnetic sublattices are composed of manganese, and establish MRG as a versatile alternative to $\text{Gd}_x(\text{FeCo})_{1-x}$ for SP-AOS applications. In MRG, the Mn atoms occupy two inequivalent sub-lattices at Wyckoff positions $4a$ and $4c$ with antiferromagnetic intersublattice coupling⁷. At low temperature the magnetization of the Mn($4c$) sublattice is dominant, but as temperature increases the magnetization of Mn($4c$) falls faster than the magnetization of Mn($4a$) leading to a compensation temperature T_{comp} where the two are equal and opposite as the net magnetization crosses zero¹⁹. The value of T_{comp} can be varied by changing Ru concentration, so it is possible to make MRG peculiarly insensitive to external magnetic fields by decreasing its magnetisation²⁰. The electronic structures of the two sublattices are different. There is a spin gap in MRG at or near the Fermi energy: the Mn($4c$) electrons have a high spin-polarized density of states whereas that of the Mn($4a$) electrons is lower or even zero. The unusual electronic structure accounts for an anomalous Hall effect (AHE) and a magneto-optical Kerr effect (MOKE) that are greater than those seen in common ferromagnets, even at T_{comp} ^{20,21}, because both AHE and MOKE probe mainly the spin-

polarized conduction band associated with Mn in the 4c position. The domains can be directly imaged in the Kerr microscope regardless of the net magnetization value²².

In our experiments, we investigated SP-AOS in 19 MRG thin films with different Ru contents and T_{comp} below or above room temperature (RT). The films are deposited on MgO (100) substrates, which leads to a slight tetragonal distortion of the cubic XA-type structure (from space group 216 - $F\bar{4}3m$ to space group 119 - $I4m2$), which is responsible for the perpendicular magnetic anisotropy of the MRG films. Optical pulses of 200 fs duration and 800 nm wavelength were generated by a mode-locked Ti-sapphire laser seeding a 1 kHz amplifier. Figure 1a displays the result of irradiating a Mn_2RuGa film by a single 200 fs pulse with Gaussian intensity profile, as observed by *ex situ* Kerr microscopy. Here the light or dark contrast indicates an up or down orientation of the Mn(4c) sublattice in the out-of-plane direction. For either initial magnetization direction, after the action of a single laser pulse, we observe the formation of a domain with switched magnetization in the irradiated area. As the irradiation power is increased to 3 μJ as shown in Fig 1b, a multidomain patterns appears in the center of the irradiated zone where the temperature has transiently exceeded the Curie temperature of the sample ($\sim 500\text{ K}$)⁷ leading to thermal demagnetization, and remagnetization in sub-micron domains of size close to the resolution of the Kerr microscope. They are much smaller than those normally observed at room temperature during the reversal process after saturating the magnetization ($\sim 100\ \mu\text{m}$). It is established that such temperatures are reached in the very first picoseconds following an optical excitation in transition metal compounds¹², after which the system remagnetizes randomly in the stray field during the cool down. The multidomain pattern is directly surrounded by a ring shaped switched domain, which suggests that the SP-AOS requires an incomplete but significant transient demagnetization. Interestingly,

we never observed SP-AOS in any of the MRG films having T_{comp} below RT (see Supplementary Information III). It is important to note that the observed sequence of switching originates solely from laser induced heating, which is independent of the polarization of the laser pulse. To verify this we repeated the experiment with circularly polarized laser pulses of opposite helicities (not shown). The SP-AOS occurred identically for both helicities, which eliminates the possibility of any contribution from magnetic circular dichroism²³. On further increasing the laser power to 5 μJ , the center of the irradiated spot on the film is ablated.

Figure 2a depicts the results of the irradiation of 1 to 5 successive laser pulses on $\text{Mn}_2\text{Ru}_{1.0}\text{Ga}$. The panels show different regions that were subjected to the given numbers of shots. Consistently, the irradiation by a series of laser pulses leads to a toggling of the direction of the magnetization, which was observed for up to 12 consecutive pulses. As indicated earlier, the effect was observed in MRG samples provided T_{comp} was above RT. The outcome of SP-AOS attempts in various other MRG samples with T_{comp} below RT is presented in Supplementary Information III. A thin rim surrounding the switched domains was systematically observed in our experiments. Although tiny drift of the laser pulse between consecutive pulses could account for this rim in some cases, the rim is sometimes seen to be formed of a multidomain pattern (see Fig. 2a). This observation is further confirmed in Fig. 2b, where a magnetization pattern with small domains is caused by sweeping the surface with a 1 kHz train of pulses. A few deterministically switched areas are observed at the end-point of the beam scan, caused by the vibration of the stage at the end of the motion. This multidomain pattern is rather unexpected and it is the consequence of sweeping the multidomain rim, as sketched in Fig. 2c. This point is important for two reasons. First of all, helicity dependent AOS (HD-AOS) is an alternative approach to switching the magnetization of ferrimagnetic and ferromagnetic

materials. The HD-AOS method relies on a train of tens to thousands of femtosecond pulses with precisely-defined energy, and it is commonly observed as a narrow ring surrounding a thermally demagnetized area at the center of the impact area of a laser pulse²⁴⁻²⁶. For convenience, HD-AOS is usually demonstrated by i) sweeping a train of circularly polarized pulses on a magnetic surface, which causes the switching of a large magnetic area and ii) imaging the result by magneto-optical microscopy. In view of our result, such an approach should preclude the identification of a new material with SP-AOS as we showed in Fig.2b that sweeping the laser beam can lead to full demagnetization of the sample irrespective of the light polarization (see also Supplementary Information V). Secondly the multidomain pattern in Fig. 2b was obtained without ever reaching the Curie temperature. Instead, it relies on the existence of a stochastic mechanism at the SP-AOS fluence threshold.

MRG possesses a low net magnetization and a high anisotropy field. Therefore, the coercive field of MRG films is usually superior to 0.2 T and can reach values as high as 10 T²⁰ when the temperature is very close to T_{comp} . It is interesting to see whether a highly-coercive sample can be switched by light at RT. Figure 3 shows the toggling of magnetization following a sequence of pulses in a thin layer of $\text{Mn}_2\text{Ru}_{0.75}\text{Ga}$ with coercivity exceeding 1 T. That sample could not be saturated with an electromagnet and it was therefore measured in its virgin state, which is characterized by a distribution of magnetic domains with a predominance of magnetization directed toward the substrate. Toggling of individual domains can be observed although the sample cannot be switched by the external magnetic field of ~1 T. The SP-AOS observed in samples with compensation temperature close to RT is particularly important for a two reasons: 1) the threshold energy required to accomplish SP-AOS is small compared to that of samples having T_{comp} far above RT. 2) Close to T_{comp} , the coercivity of MRG is high, which

makes it difficult to erase the written domains. In other words, these samples are ideal for non-volatile magnetic memory, where the data needs to be very stable against external magnetic perturbations.

Density functional theory calculation can provide an estimate of the spin- and site-resolved densities of states (DOS)^{27,28}. Such calculations show that the 3*d* moments of the Mn(4*a*) and Mn(4*c*) sublattices are antiferromagnetically coupled and their spins are oppositely oriented. Moreover, the DOS of one spin direction exhibits a band gap ~1 eV close to the Fermi level that is absent for the opposite spin direction, which made MRG the first example of a half-metallic compensate⁷. The high spin polarization at the Fermi level, arising mainly from the 4*c* sublattice, accounts for the strength of the AHE and MOKE. This ground-state DOS provides a starting point to discuss the origin of the SP-AOS in MRG²⁹, although the energy bands do not represent the temperature-dependence of the magnetization of the two sublattices. On-site electronic correlations and local moments contribute to a local spin splitting of the DOS that persists above the Curie temperature in 3*d* metals. The 800 nm (1.5 eV) laser pulse corresponds to a frequency of $3.6 \cdot 10^{14}$ Hz, and a period of 3 fs. It is expected to disrupt the inter-atomic, intersite exchange (<0.1 eV) and rapidly destroy the magnetic order; most of the corresponding angular momentum is transferred to the lattice³⁰. The intra-atomic, on-site exchange depends on stronger Coulomb interactions (3 – 5 eV) which will not be completely destroyed, so the switching involves reassembly of magnetic order from the excited atomic moments, which in a ferrimagnet could include effects of spin and charge transfer between sites¹⁹.

An essential requirement for toggle switching is that some marker of the original spin direction must persist to act as a seed for the reassembled magnetic order, albeit in the opposite direction. The currently accepted explanation of the effect in $\text{Gd}_x(\text{Fe,Co})_{100-x}$ depends on a

demagnetizing time for Gd (~ 1.5 ps) that is about five times slower than that of Fe (~ 300 fs)³. The slowly demagnetizing gadolinium loses spin to the already demagnetized iron resulting in a transient ferromagnetic state, which the growing iron moment transforms into a ferrimagnetic state by flipping the Gd sublattice. The intra-sublattice Fe-Fe exchange is the dominant exchange interaction, over-riding the Gd-Fe exchange. The new switched magnetizations of both sublattices then build up on this reversed template.

The picture in MRG is rather different. Assuming that the more rapidly demagnetized sublattice is $4c$, because it has the greater DOS at the Fermi level and a maximum in the unoccupied density of states about 1.2 eV higher in energy, the $4a$ sites would play the part of Gd. But in MRG the $4a$ intrasublattice exchange is the strongest interatomic exchange interaction (The exchange fields deduced from an analysis of the high-field magnetization in a film with a compensation temperature of 150 K are $B_{aa} = 786$ T, $B_{cc} = 293$ T and $B_{ac} = -343$ T)³¹. The slowly-demagnetizing $4a$ sublattice could remagnetize the $4c$ spins parallel to it, but magnetocrystalline anisotropy (strongly easy axis on $4c$, but weak on $4a$) may then decide which of them flips to form the template for the new ferrimagnetic state. The flaw in any such argument is that it is based on the magnetic properties of the atoms in their ground state, whereas the details of the switching depend on the atomic moments and exchange interactions in their transient excited states, which are unknown.

The much narrower intensity window observed for SP-AOS at 400 nm than at 800 nm suggests that weakening of on-site electron correlations with the higher energy excitation (3.0 eV) makes it much more difficult to fulfill the conditions necessary for toggle switching. The proximity to the plasma cut-off would imply that the pulse energy is transferred to other degrees

of freedom to a larger extent *i.e.* the amount of excited electrons from the vicinity of the Fermi energy would become smaller.

Regarding the timescale for switching in MRG, the sublattice demagnetizing time is on the order of 1 ps³², and we found that the remagnetizing time of the MRG film on the MgO substrate was found to be about 100 times longer. Here we speculate that the ultra-fine domain structure seen when the films are heated above their Curie point might be an image of frozen-in critical fluctuations.

There remains the question of the role of the compensation point. Is it enough to be close to compensation as Mangin and co-workers suggest¹⁶, or is it somehow necessary to cross compensation to achieve switching?

A simplified representation of the effect of a laser pulse excitation on DOS for initial temperature on either side of T_{comp} is displayed in Fig. 4. In that picture we assume a 100% spin polarization, with the Fermi level in the spin gap. Figs 4a,b sketch the DOSs before excitation when T_{comp} is below or above RT. The temperature variation of the sublattice magnetization is taken into account insofar as the majority and minority spin subbands are interchanged. In the first case, Fig 4a, the magnetization of the Mn(4a) sublattice is dominant and the main effect of the laser pulse is to excite mainly Mn(4c) electrons at the Fermi level and promote them to unoccupied states ~1.5 eV higher in energy, that are also mainly of 4c character. After reassembly, the 4c moments are still antiparallel to the largely unscathed 4a sublattice and no switching has occurred.

In the second case, Fig. 4b, it is the now majority-spin Mn(4c) electrons at the Fermi level that are excited, rapidly reducing the 4c atomic moments so that the Mn(4a) sublattice

becomes momentarily dominant. Provided some vestige of the original order persists in the core or excited states to create an effective field, B_{eff} , the net magnetization flips and the moments reassemble in the switched configuration.

Toggle switching is not seen in iron or nickel, which have a single ferromagnetic lattice, because 1.5 eV laser pulses excite sufficient electron of *both* spins to effectively disorder the entire atomic moments.

In summary, we have reported the experimental demonstration of SP-AOS in half-metallic compensated ferrimagnetic MRG films, where the both magnetic sublattices are composed of manganese, occupying crystallographic different sites. These results extend the scope of the phenomenon beyond a limited range of $\text{Gd}_x(\text{Fe,Co})_{100-x}$ amorphous alloys with $x \approx 25$, where the magnetic sublattices are defined chemically. The Heusler alloys are a huge family, with an established body of knowledge about their magnetic and electronic properties that will allow us to advance our understanding of the SP-AOS phenomenon by designing new materials that could be the basis of future optically-controlled magnetic devices. Beyond the newly-demonstrated quality of MRG as an optomagnetic material, its large intrinsic spin-orbit torque, which relies on the absence of inversion symmetry of the Mn(4c) sublattice^{32,333,343} opens prospects for new multifunctionality. Therefore, MRG and its chemically tailored successors offer the prospects of both new insights into condensed matter on a femtosecond timescale and new technological prospects.

Methods: MRG films with different Ru content were grown on MgO(001) substrates by DC magnetron sputtering at 250°C substrate temperature in a Shamrock system with a base pressure of 2×10^{-8} Torr. They were co-sputtered from Ru and stoichiometric Mn₂Ga targets. The Ru concentration was controlled by varying the Mn₂Ga target plasma power while fixing the Ru one. The samples were then capped with a protective layer of 2 nm of Al₂O₃.

Femtosecond laser pulses were generated by Ti-sapphire laser seeding a 1 kHz amplifier with a Q-switched cavity. Their central wavelength was 800 nm and the pulse duration was about 200 fs. The amplifier can be operated in continuous mode where a train of pulses is generated at a repetition rate of 1 kHz or in single pulse mode where the emission of one single pulse can be externally triggered. In some cases, 400 nm laser pulses were obtained by second harmonic generation in a β -BaB₂O₄ crystal.

Prior to laser irradiation, the films were saturated in the maximum 1 T perpendicular magnetic field of our Evico Kerr microscope. Different locations on the sample were then irradiated with several linearly polarized laser pulses of different powers, followed by ex-situ imaging of the final magnetic in a magneto-optical Kerr microscope.

Figure 1: Single-pulse all-optical switching (SP-AOS) in Mn_2RuGa . **a.** Irradiation at low energy showing the switching of the magnetization. **b.** Increasing the irradiation energy leads to the development of a thermally demagnetized area in the center of the irradiated area where the fluence is the highest.

Figure 2: Toggling of magnetization in Mn_2RuGa . **a.** Magnetization pattern as a function of the number of applied pulses. **b.** Multi-domain pattern obtained by sweeping a 1 kHz train of pulses on the surface of the sample. **c.** Schematic of the demagnetization obtained by sweeping a multiple-pulse beam across a sample.

Figure 3: Toggling of magnetization in a high-coercivity Mn_2RuGa film. Toggling of the micron-scale domains of a sample in a virgin state is observed with repeated pulses. There is a net imbalance of domains pointing in and out of the plane.

Figure 4: Representation of the switching mechanism in MRG. Schematic density of states taking spin disorder into account **a.** when the compensation temperature T_{comp} is below RT and **b.** when T_{comp} is above RT. The 1.5 eV laser pulse excites electrons from near the Fermi level to higher, unoccupied states in the band and further disorders the atomic moments. In **a.** they relax to the same room-temperature configuration they started from, but in **b.** a residual effective field B_{eff} in the original direction of magnetization reverses the reduced net magnetization, relabeling the sub-bands and the moments relax to a reversed room-temperature state.

References

1. Kimel, A. V. & Li, M. Writing magnetic memory with ultrashort light pulses. *Nat. Rev. Mater.* **4**, 189–200 (2019).
2. Lalieu, M. L. M., Lavrijsen, R. & Koopmans, B. Integrating all-optical switching with spintronics. *Nat. Commun.* **10**, 110 (2019).
3. Radu, I. *et al.* Transient ferromagnetic-like state mediating ultrafast reversal of antiferromagnetically coupled spins. *Nature* **472**, 205–209 (2011).
4. Lalieu, M. L. M., Peeters, M. J. G., Haenen, S. R. R., Lavrijsen, R. & Koopmans, B. Deterministic all-optical switching of synthetic ferrimagnets using single femtosecond laser pulses. *Phys. Rev. B* **96**, 220411(R) (2017).
5. Iihama, S. *et al.* Single-Shot Multi-Level All-Optical Magnetization Switching Mediated by Spin Transport. *Adv. Mater.* **30**, 1804004 (2018).
6. Gorchon, J. *et al.* Single shot ultrafast all optical magnetization switching of ferromagnetic Co/Pt multilayers. *Appl. Phys. Lett.* **111**, 042401 (2017).
7. Kurt, H. *et al.* Cubic Mn₂Ga Thin Films: Crossing the Spin Gap with Ruthenium. *Phys. Rev. Lett.* **112**, 027201 (2014).
8. Jungwirth, T., Marti, X., Wadley, P. & Wunderlich, J. Antiferromagnetic spintronics. *Nat. Nanotechnol.* **11**, 231–241 (2016).
9. Baltz, V. *et al.* Antiferromagnetic spintronics. *Rev. Mod. Phys.* **90**, 015005 (2018).
10. Němec, P., Fiebig, M., Kampfrath, T. & Kimel, A. V. Antiferromagnetic opto-spintronics. *Nat. Phys.* **14**, 229–241 (2018).
11. Kirilyuk, A., Kimel, A. V. & Rasing, Th. Ultrafast optical manipulation of magnetic order. *Rev. Mod. Phys.* **82**, 2731–2784 (2010).

12. Beaurepaire, E., Merle, J.-C., Daunois, A. & Bigot, J.-Y. Ultrafast Spin Dynamics in Ferromagnetic Nickel. *Phys. Rev. Lett.* **76**, 4250–4253 (1996).
13. Ostler, T. A. *et al.* Ultrafast heating as a sufficient stimulus for magnetization reversal in a ferrimagnet. *Nat. Commun.* **3**, 666 (2012).
14. Wienholdt, S., Hinzke, D., Carva, K., Oppeneer, P. M. & Nowak, U. Orbital-resolved spin model for thermal magnetization switching in rare-earth-based ferrimagnets. *Phys. Rev. B* **88**, 020406(R) (2013).
15. El Hadri, M. S. *et al.* Two types of all-optical magnetization switching mechanisms using femtosecond laser pulses. *Phys. Rev. B* **94**, 064412 (2016).
16. Xu, Y. *et al.* Ultrafast Magnetization Manipulation Using Single Femtosecond Light and Hot-Electron Pulses. **29**, 1703474 (2017).
17. Vomir, M., Albrecht, M. & Bigot, J.-Y. Single shot all optical switching of intrinsic micron size magnetic domains of Pt/Co/Pt ferromagnetic stack. **111**, 242404 (2017).
18. Stupakiewicz, A., Szerenos, K., Afanasiev, D., Kirilyuk, A. & Kimel, A. V. Ultrafast nonthermal photo-magnetic recording in a transparent medium. *Nature* **542**, 71 (2017).
19. Betto, D. *et al.* Site-specific magnetism of half-metallic Mn_2Ru_x thin films determined by x-ray absorption spectroscopy. *Phys. Rev. B* **91**, 094410 (2015).
20. Thiyagarajah, N. *et al.* Giant spontaneous Hall effect in zero-moment $\text{Mn}_2\text{Ru}_x\text{Ga}$. *Appl. Phys. Lett.* **106**, 122402 (2015).
21. Fleisher, K. *et al.* Magneto-optic Kerr effect in a spin-polarized zero moment ferrimagnet. *Phys. Rev. B* **98**, 134445 (2018).
22. Siewierska, K. E., Teichert, N., Schäffer, R. & Coey, J. M. D. Imaging Domains in a Zero-Moment Half Metal. *IEEE Trans. Magn.* **55**, 2600104 (2019).

23. Khorsand, A. R. *et al.* Role of Magnetic Circular Dichroism in All-Optical Magnetic Recording. *Phys. Rev. Lett.* **108**, 127205 (2012).
24. Stanciu, C. D. *et al.* All-Optical Magnetic Recording with Circularly Polarized Light. *Phys. Rev. Lett.* **99**, 047601 (2007).
25. Mangin, S. *et al.* Engineered materials for all-optical helicity-dependent magnetic switching. *Nat. Mater.* **13**, 286–292 (2014).
26. Lambert, C.-H. *et al.* All-optical control of ferromagnetic thin films and nanostructures. *Science* **345**, 6202 (2014).
27. Galanakis, I., Özdoğan, K., Şaşıoğlu, E. & Blügel, S. Effect of disorder on the magnetic properties of cubic $\text{Mn}_2\text{Ru}_x\text{Ga}$ compounds: A first-principles study. *J. Appl. Phys.* **116**, 033903 (2014).
28. Žic, M. *et al.* Designing a fully compensated half-metallic ferrimagnet. *Phys. Rev. B* **93**, 140202(R) (2016).
29. Elliott, P., Müller, T., Dewhurst, J. K., Sharma, S. & Gross, E. K. U. Ultrafast laser induced local magnetization dynamics in Heusler compounds. *Sci. Rep.* **6**, 38911 (2016).
30. Dornes, C. *et al.* The ultrafast Einstein-de Haas effect. **565**, 209–212 (2017).
31. Fowley, C. *et al.* Magnetocrystalline anisotropy and exchange probed by high-field anomalous Hall effect in fully compensated half-metallic $\text{Mn}_2\text{Ru}_x\text{Ga}$ thin films. *Phys. Rev. B* **98**, 220406(R) (2018).
32. Bonfiglio, G. *et al.* Magnetisation dynamics of the compensated ferrimagnet $\text{Mn}_2\text{Ru}_x\text{Ga}$. *Rev.*
33. Lenne, S. *et al.* Giant spin-orbit torque in a single ferrimagnetic metal layer. *arXiv* 1903.04432 (2019).

34. Finley, J., Lee, C.-H., Huang, P. Y. & Liu, L. Spin-Orbit Torque Switching in a Nearly Compensated Heusler Ferrimagnet. *Adv. Mater.* **31**, 1805361 (2019). 1903.04432 (2019).

Author contributions:

C. B., J. B. and J. M. D. C. designed the project. Experimental work was done by C. B., N. T. and J. B.. Growth and characterization of the samples were carried out by G. A. and K. S.. Numerical simulations were performed by Z. G. and J. B.. C. B., J. B., P. S. and K. R. interpreted the data. All authors discussed the results. C. B., J. B. and J. M. D. C. wrote the paper.

Acknowledgements:

This project has received funding from Science Foundation Ireland through contracts 16/IA/4534 ZEMS and 12/RC/2278 AMBER and from the European Union's FET-Open research programme under grant agreement No 737038. C.B. is grateful to Irish Research Council for her post-doctoral fellowship. N. T. would like to acknowledge funding from the European Union's Horizon 2020 research and innovation programme under the Marie Skłodowska-Curie EDGE grant agreement No 713567.

The authors declare no competing financial interest.

Figure 1

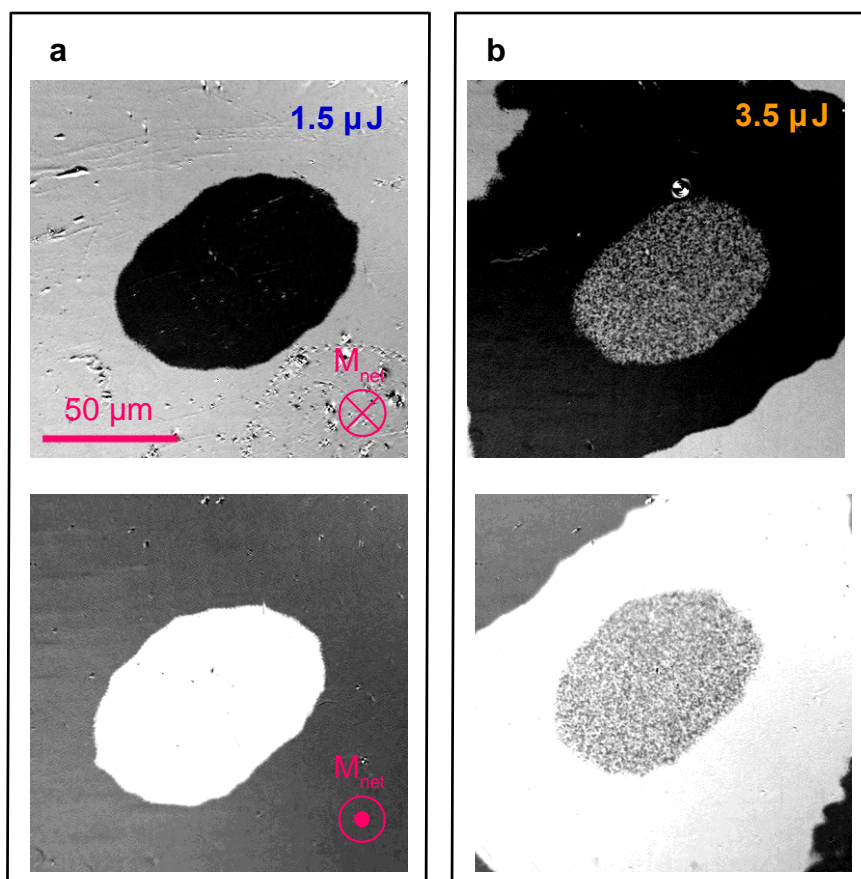


Figure 2

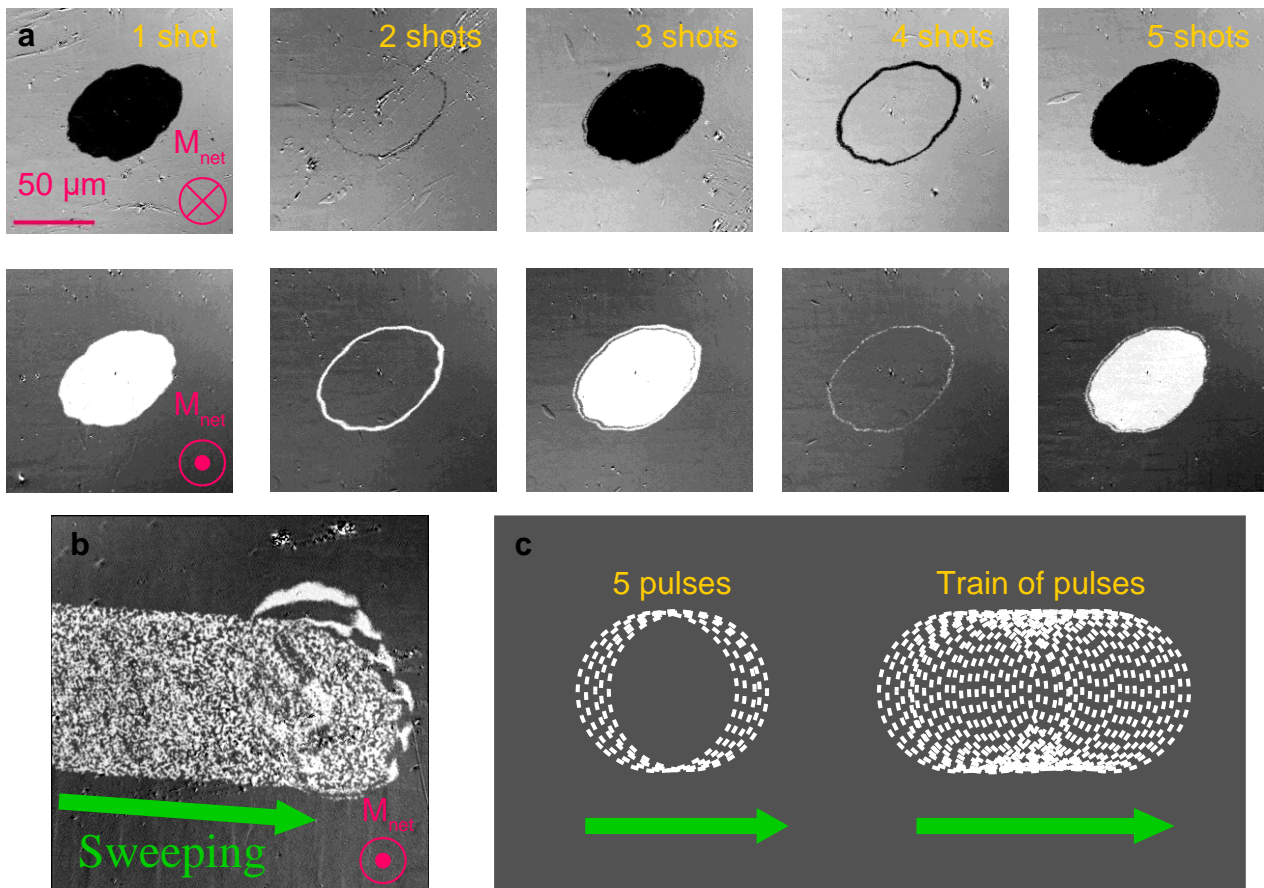


Figure 3

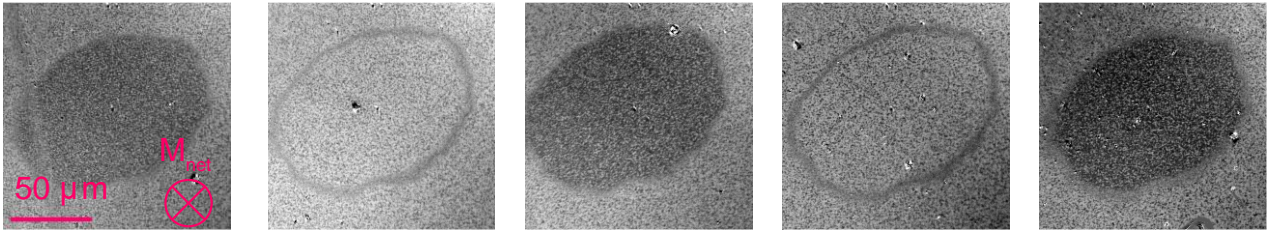
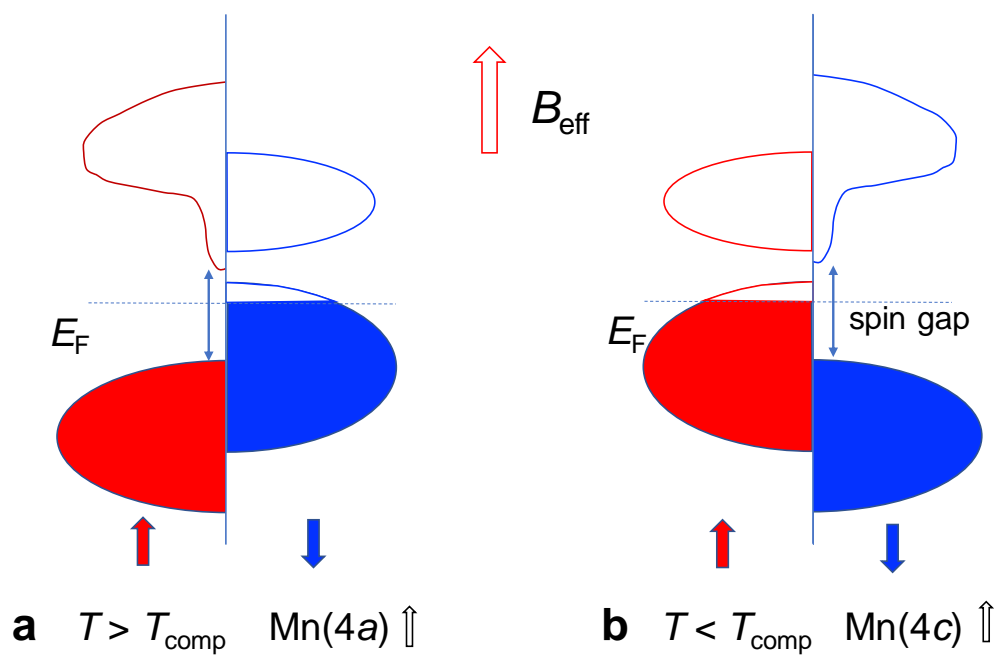


Figure 4



Supplementary Information

Single pulse all-optical toggle switching of magnetization without Gd: The example of $\text{Mn}_2\text{Ru}_x\text{Ga}$

C. Banerjee, N. Teichert, K. Siewierska, Z. GerCSI, G. Atcheson, P. Stamenov,
K. Rode, J. M. D. Coey and J. Besbas*

¹ CRANN, AMBER and School of Physics, Trinity College, Dublin 2, Ireland

[*besbasj@tcd.ie](mailto:besbasj@tcd.ie)

I. STRUCTURAL AND MAGNETIC CHARACTERIZATION OF $\text{Mn}_2\text{Ru}_{1.0}\text{Ga}$

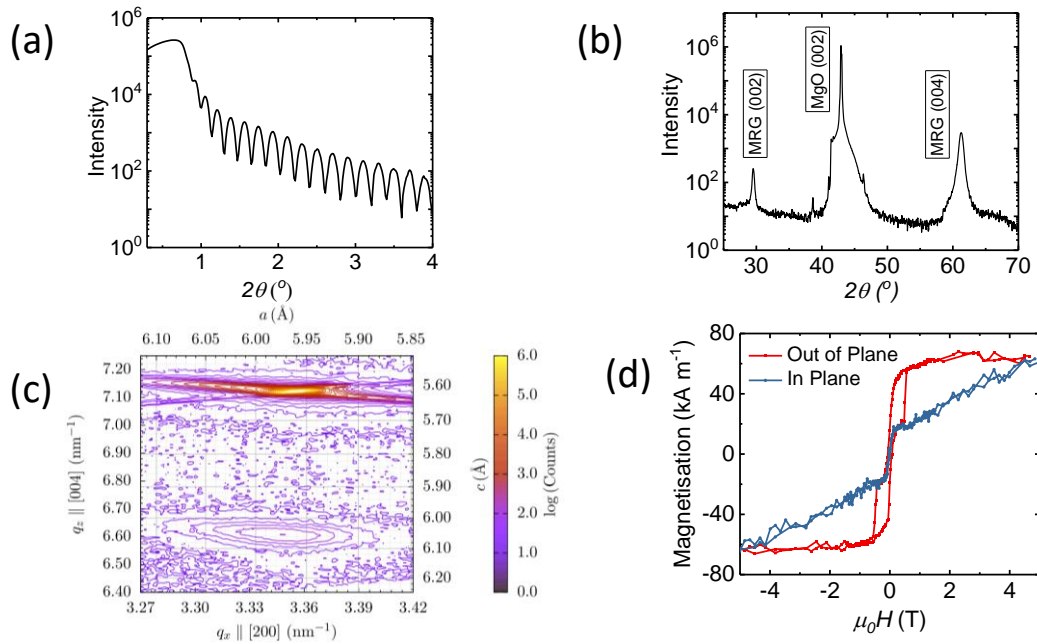


Figure S1: Characterisation of $\text{Mn}_2\text{Ru}_{1.0}\text{Ga}$ (MRG): (a) X ray reflectivity pattern of the MRG thin film. Fitting gives a thickness of 42.76 nm and a density of 8.2 g cm⁻³, (b) X ray diffraction pattern of MRG thin film on MgO (001) substrate. (c) Reciprocal space map of MgO (113) peak and MRG (204) peak with lattice parameters calculated with respect to the MRG unit cell and (d) magnetisation versus field applied in plane and out of plane with respect to the MRG film at 300 K.

X-ray data on the films are shown in Fig. S1 (a), (b) and (c). X-ray reflectivity (XRR) pattern shown in Fig. S1 (a) has been fitted using X'Pert Reflectivity software and the film thickness was calculated to be 42.76 nm. The X-ray diffraction (XRD) pattern in Fig. S1 exhibits (002) and (004) reflections from the MRG, together with peaks from the MgO substrate. The c -parameter is calculated by applying the Bragg formula to the (004) reflection and was hence found to be 604.7 pm. Reciprocal space map (RSM) of the MRG film shown in Fig. S1 (c) confirms the c -parameter obtained from XRD, and shows a distribution of a -parameters around the central value of 595.8 pm, which corresponds to that of MgO. This also demonstrates how substrate strain induces a $\sim 1\%$ tetragonal elongation of the MRG unit cell since the c/a ratio is 1.01, giving rise to perpendicular magnetic anisotropy (PMA). SQUID magnetometry data in Fig. S1 (d) shows the magnetization dependence of field applied out of plane and in plane at 300 K relative to the surface of the thin film. The coercivity (H_C) of the sample is 0.48 T and saturation magnetisation is 65 kAm^{-1} . The soft component in the out of plane data as well as the small in plane component in the magnetisation is thought to originate from the non-collinearity of the two antiferromagnetically coupled Mn magnetic sublattices¹.

II. MEASUREMENT OF OPTICAL AND TRANSPORT MAGNETOMETRY OF $\text{Mn}_2\text{Ru}_{1.0}\text{Ga}$

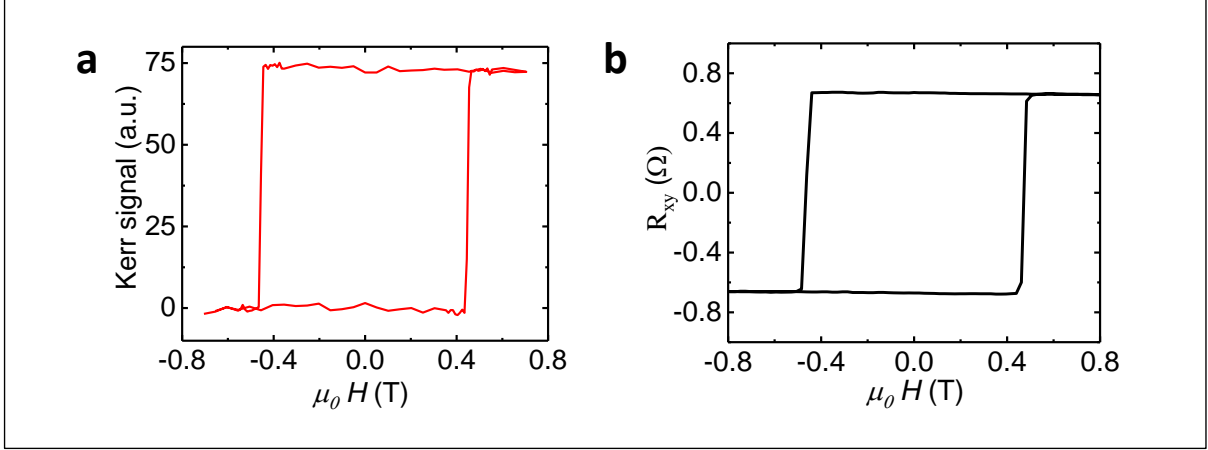


Figure S2: Measured hysteresis loops of $\text{Mn}_2\text{Ru}_{1.0}\text{Ga}$ via (a) Kerr microscopy and (b) anomalous Hall effect.

We have also measured the magnetic hysteresis loop using Polar Kerr effect and anomalous Hall effect in the perpendicular $\text{Mn}_2\text{Ru}_{1.0}\text{Ga}$ film which are compared in Fig. S2. In contrast to the two step switching observed in the Squid loop (See Fig. S1d), here the hysteresis exhibits straightforward switching behaviour with an average switching field of 460 mT in both cases. Whereas the Squid probes the net magnetic moment, the measurement in optical and electrical transport, on the other hand, relies on the distribution of spin resolved electrons at the Fermi energy, which in MRG reflects the 4c sublattice magnetization. Consequently, the hysteresis shown in Fig. S2 as well as the domain images presented here reflects the local magnetization state of the 4c sublattice. It is therefore possible to explore the local magnetization state even at compensation.

III. RESULT OF PULSE ENERGY DEPENDENT MEASUREMENT IN MRG SAMPLE WHERE AOS WAS NOT OBSERVED

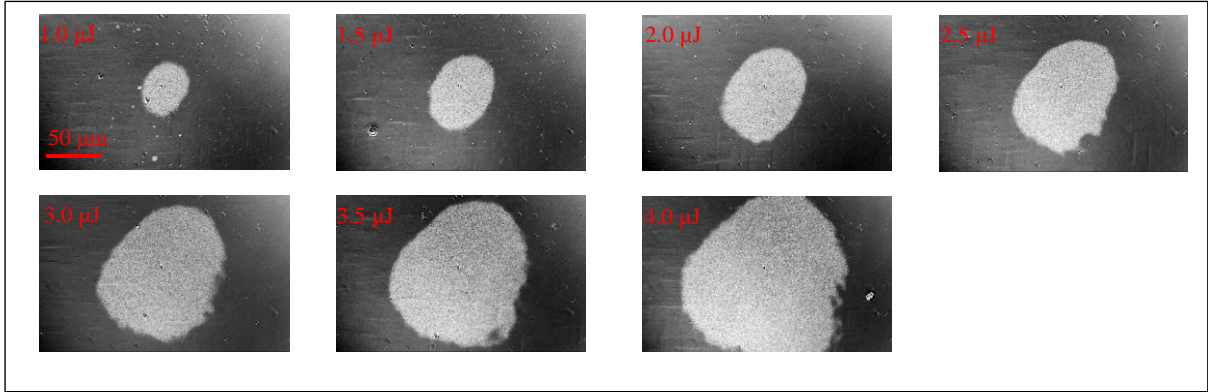


Figure S3: Typical Kerr microscope images of MRG after single laser pulse of various powers were irradiated on different positions of the surface. The results show a multidomain pattern has formed.

In the main text, single pulse all optical switching (AOS) is presented for MRG samples having T_{comp} above room temperature. Nevertheless, such toggling was not observed for the MRG samples having T_{comp} below room temperature. Figure S3 shows typical Kerr micrographs after the pulse energy dependent measurement in such a film. The results reveal the presence of multidomain state with an onset at $\sim 1 \mu\text{J}$ of laser energy. This is contrary to the $\text{Mn}_2\text{Ru}_{1.0}\text{Ga}$ results, where a ring of switched domain was observed around the thermally demagnetized region.

IV. SP-AOS MEASUREMENT ON $\text{Mn}_2\text{Ru}_{0.92}\text{Ga}$ USING LASER PULSES OF WAVELENGTH 400 NM

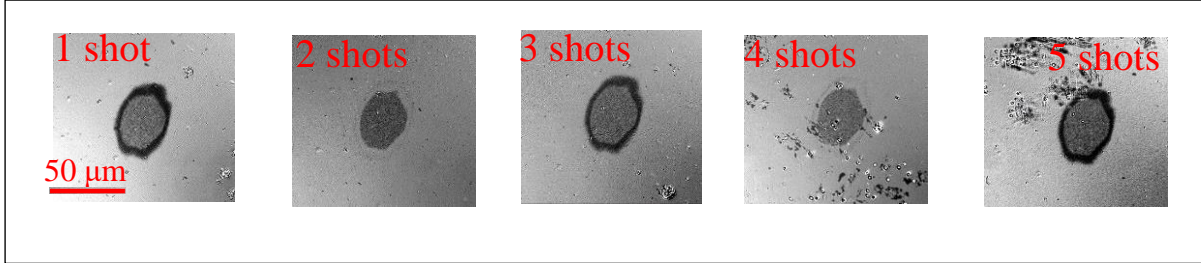


Figure S4: Single pulse all optical switching measurement performed on $\text{Mn}_2\text{Ru}_{0.92}\text{Ga}$ using laser pulses of wavelength 400 nm and pulse energy 900 nJ. The number of laser pulses the region is exposed to is labelled in each image.

In order to substantiate the thermal origin of SP-AOS in MRG, we examined the response of the magnetization of $\text{Mn}_2\text{Ru}_{0.92}\text{Ga}$ to the laser pulses of different wavelength and polarization. In Fig. S4 the response is shown for a laser light of wavelength 400 nm upto five laser pulses. The results are in line with the observation with 800nm (See Fig. 2 in main text). Essentially, a decrease in the excitation wavelength decreases the laser spot size, thereby increasing the thermal gradient across it. This directly affects the magnetization profile of the irradiated region and the switching is observed in a relatively narrower ring as compared to the 800 nm case around the thermally demagnetized area.

V. EFFECT OF CIRCULARLY POLARIZED LASER PULSES ON AOS OF MRG

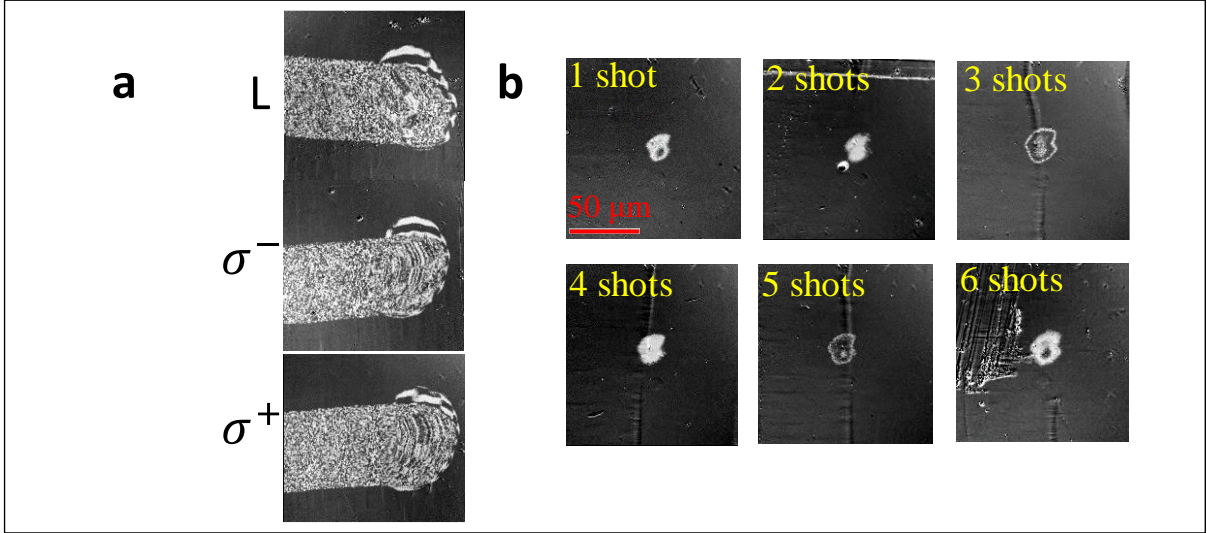


Figure S5: Magneto-optical image of the domain pattern in $\text{Mn}_2\text{Ru}_{1.0}\text{Ga}$ sample obtained (a) after sweeping a train of laser pulses of pulse repetition rate 1 kHz having linear (L), left-circular (σ^-) and right-circular (σ^+) polarization (b) after the impact of N ($N=1\dots6$) left circularly polarized laser pulses of energy 800 nJ irradiated at different positions of the sample. The number of laser pulses the region is exposed to is labelled in each image.

As mentioned in the main text, we did not find any dependence of the magnetization response of MRG on the light helicity, which is shown in Fig. S5. In earlier reports, helicity dependent AOS (HD-AOS) using circular polarization have been studied by sweeping a train of laser pulses across the magnetic film, where deterministic switching was seen as a ring of switched domain around a thermally demagnetized area^{2,3}. In our case, the formation of multidomain pattern was observed, which was however not surrounded by any switched region, irrespective of the light helicity (See Fig. S5a). In fact, this multidomain pattern arises from the multidomain rim formed around the switched domain after laser pulse impact, which is described in the main text. Clearly, this multidomain formation occurs at the threshold fluence required for SP-AOS and exhibits stochastic switching behaviour upon the action of laser pulses. This feature is shown in Fig. S5b, where the impact of a left circularly polarized laser is shown for up to six pulses, at a threshold laser energy where AOS is visible. The characteristic of this random switching solely belongs to the low laser power and independent of the light helicity.

TABLE S1: Outcome of SP-AOS attempt in various MRG samples. In some cases, where similar behaviour was found for films with similar composition, only one entry is shown. The T_{comp} s shown in black are experimentally measured by SQUID, while the remaining (shown in red) are interpolated.

| Sample | T_{comp} | Coercive Field | Switching Observed? |
|---------------------------------------|-------------------|----------------|---------------------|
| Mn ₂ Ru _{0.5} Ga | 75 K | 150 mT | No |
| Mn ₂ Ru _{0.55} Ga | 80 K | 170 mT | No |
| Mn ₂ Ru _{0.62} Ga | 130 K | 260 mT | No |
| Mn ₂ Ru _{0.67} Ga | 145 K | 350 mT | No |
| Mn ₂ Ru _{0.68} Ga | 160 K | 370 mT | No |
| Mn ₂ Ru _{0.7} Ga | 165 K | 440 mT | No |
| Mn ₂ Ru _{0.8} Ga | 245 K | 740 mT | No |
| Mn ₂ Ru _{0.9} Ga | 300 K | > 1 T | Yes |
| Mn ₂ Ru _{0.92} Ga | 315 K | >1 T | Yes |
| Mn ₂ Ru _{0.93} Ga | 320 K | >1 T | Yes |
| Mn ₂ Ru _{0.94} Ga | 325 K | >1 T | Yes |
| Mn ₂ Ru _{0.95} Ga | 375 K | 600 mT | Yes |
| Mn ₂ Ru _{1.0} Ga | 400 K | 480 mT | Yes |

References:

1. Fowley, C. *et al.* Magnetocrystalline anisotropy and exchange probed by high-field anomalous Hall effect in fully compensated half-metallic $\text{Mn}_2\text{Ru}_x\text{Ga}$ thin films. *Phys. Rev. B* **98**, 220406(R) (2018).
2. Mangin, S. *et al.* Engineered materials for all-optical helicity-dependent magnetic switching. *Nature Mater.* **13**, 286–292 (2014).
3. Lambert, C.-H. *et al.* All-optical control of ferromagnetic thin films and nanostructures. *Science* **345**, 6202 (2014).